



# HHS Public Access

Author manuscript

*Nat Biotechnol.* Author manuscript; available in PMC 2009 November 10.

Published in final edited form as:

*Nat Biotechnol.* 2008 December ; 26(12): 1373–1378. doi:10.1038/nbt.1507.

## Integrated Blood Barcode Chips

**Rong Fan**<sup>1,2,3,5</sup>, **Ophir Vermesh**<sup>1,2,3,5</sup>, **Alok Srivastava**<sup>1,4</sup>, **Brian K.H. Yen**<sup>1,2,3</sup>, **Lidong Qin**<sup>1,2,3</sup>, **Habib Ahmad**<sup>1,2,3</sup>, **Gabriel A. Kwong**<sup>1,2,3</sup>, **Chao-Chao Liu**<sup>1,2,3</sup>, **Juliane Gould**<sup>1,2,3</sup>, **Leroy Hood**<sup>1,4</sup>, and **James R. Heath**<sup>1,2,3,\*</sup>

<sup>1</sup>NanoSystems Biology Cancer Center(NSBCC), California Institute of Technology, Pasadena, California

<sup>2</sup>Kavli Nanoscience Institute, California Institute of Technology, Pasadena, California

<sup>3</sup>Division of Chemistry and Chemical Engineering, California Institute of Technology, Pasadena, California

<sup>4</sup>Instititue for Systems Biology, Seattle, Washington

### Abstract

Blood comprises the largest version of the human proteome<sup>1</sup>. Changes of plasma protein profiles can reflect physiological or pathological conditions associated with many human diseases, making blood the most important fluid for clinical diagnostics<sup>2-4</sup>. Nevertheless, only a handful of plasma proteins are utilized in routine clinical tests. This is due to a host of reasons, including the intrinsic complexity of the plasma proteome<sup>1</sup>, the heterogeneity of human diseases and the fast kinetics associated with protein degradation in sampled blood<sup>5</sup>. Simple technologies that can sensitively sample large numbers of proteins over broad concentration ranges, from small amounts of blood, and within minutes of sample collection, would assist in solving these problems. Herein, we report on an integrated microfluidic system, called the Integrated Blood Barcode Chip (IBBC). It enables on-chip blood separation and the rapid measurement of a panel of plasma proteins from small quantities of blood samples including a fingerprick of whole blood. This platform holds potential for inexpensive, non-invasive, and informative clinical diagnoses, particularly, for point-of-care.

---

Microfluidics has permitted the miniaturization of conventional techniques to enable high-throughput and low-cost measurements.<sup>6, 7</sup> Example platforms for biomolecular assays<sup>8, 9</sup> and bio-separations,<sup>10, 11</sup> including the separation of circulating tumor cells or plasma from whole blood<sup>12-14</sup> have been reported. However, microchips that integrate on-chip blood

---

Users may view, print, copy, and download text and data-mine the content in such documents, for the purposes of academic research, subject always to the full Conditions of use:[http://www.nature.com/authors/editorial\\_policies/license.html#terms](http://www.nature.com/authors/editorial_policies/license.html#terms)

\*Correspondence to J.R.H. (heath@caltech.edu).

<sup>5</sup>These authors contribute equally to this work.

#### AUTHOR CONTRIBUTIONS

R.F. developed and validated the DEAL barcode assay, measured cancer patient serum samples and analyzed all data. O.V. and B.Y. developed the blood separation chip. O.V., A.S. and L.Q. performed finger-prick blood test. R.F., O.V. A.S. H.A., G.K, C.L., and J.G. participated in the synthesis and validation of reagents, and the patterning of DNA barcode microarrays. L.H and J.R.H. designed and directed the project.

#### COMPETING INTRERESTS STATEMENT

The authors declare no competing financial interests.

separations from few-microliter quantities of blood, followed by rapid measurements of multiple plasma proteins are yet to be realized. The IBBC described herein was developed to rapidly assay a large panel of protein biomarkers *in situ*, starting from a fingerprick of whole blood. The immunoassay region of the chip is a microscopic barcode, integrated into a microfluidics channel, and customized for the detection of many proteins and/or for the quantitation of a single or few proteins over a broad concentration range. The versatility of this barcode immunoassay is demonstrated by detecting human chorionic gonadotropin (hCG) from human serum over a  $10^5$  concentration range, and by stratifying 22 cancer patients via multiple measurements of a dozen blood protein biomarkers for each patient. Finally the IBBC is utilized to assay a blood protein biomarker panel from whole human blood, with all key steps in the immunoassay executed within 10 minutes of finger-prick blood collection.

The IBBC was designed for the rapid execution of two sequential tasks: plasma separation from whole blood, and implementation of a multi-parameter protein assay. We first present an overview of the IBBC, and then discuss, sequentially, the ability to control the assay sensitivity, the extension of a single protein assay to an assay for a large panel of biomarkers, and, finally, the integration of plasma separation from whole blood, followed by the rapid measurement of a panel of protein biomarkers. Fig. 1 shows the design of an IBBC for blood separation and *in situ* protein measurement. A polydimethylsiloxane(PDMS)-on-glass chip was designed for 8-12 separate multi-protein assays to be executed sequentially, or in parallel, starting from whole blood. The plasma separation was achieved by exploiting the Zweifach-Fung effect of highly polarized blood cell flow at branch points of small blood vessels<sup>14-16</sup>. We utilized this hydrodynamic effect by flowing blood through a low-flow-resistance primary channel that has high-resistance, centimeter-long channels branching off perpendicularly (Fig 1a). As the resistance ratio is increased between the branches and the primary channel, a critical streamline moves closer to the primary channel wall adjoining the branch channels. Blood cells with a radius larger than the distance between this critical streamline and the primary channel wall are directed away from the high-resistance channels, and ~15% of the plasma is skimmed into the high-resistance channels. The remaining whole blood is directed towards a waste outlet. This component was re-designed from a previous report<sup>14</sup>. The glass base of the plasma-skimming channels is pre-patterned, prior to the microfluidics chip assembly, with a dense barcode-like array of ssDNA oligomers. A full barcode is repeated multiple times within a single plasma-skimming channel, and each barcode sequence constitutes a complete assay.

To detect proteins within the plasma-skimming channels, the DNA-encoded antibody library (DEAL) technique is employed to convert the pre-patterned ssDNA barcode microarray into an antibody microarray<sup>17</sup>. DNA-directed immobilization of antibodies provides a powerful means for spatial encoding<sup>18, 19</sup>. The sequences of all ssDNA oligomer pairs used (labeled **A/A'-M/M'**), and their corresponding antibodies, are listed in the Supplementary Table 1 and 2. To minimize cross-reactivity, these ssDNA molecules were designed *in silico* and then validated through a full orthogonality test. In that experiment, each of the complementary DNA molecules with Cy3 fluorescent label was added to a microwell containing a full primary ssDNA barcode array. The results showed only negligible cross-

hybridization signals (see Supplementary Fig. S7 on line). In the DEAL assay, each capture antibody is tagged with  $\sim 3$  copies of a single-stranded (ss)DNA oligomer that is complementary to ssDNA' oligomers that have been surface-patterned into a microscopic barcode within the immunoassay region of the chip. Flow-through of the DNA-antibody conjugates transforms the DNA microarray into an antibody microarray for the subsequent surface-bound immunoassay. Because DNA patterns are robust to dehydration and can survive elevated temperatures (80-100°C), the DEAL approach circumvents the denaturation of antibodies that can occur under typical microfluidics fabrication conditions.

A finger prick of blood represents only a few microliters of liquid, implying that the on-chip plasma separation process yields a few hundred nanoliters of plasma volume. To measure a large panel of protein biomarkers from this small volume, the ssDNA barcodes were patterned at a high density using microchannel-guided flow patterning (Supplementary §S.3 on line). The entire ssDNA bar code was patterned using a single polydimethylsiloxane (PDMS) mold that was thermally bonded onto a poly-amine coated glass slide. Polyaminated surfaces permit significantly higher DNA loading than do more traditional aminated surfaces<sup>20</sup>, and provide for an accompanying increase in assay sensitivity (see Supplementary Fig.S4 online). Different solutions, each containing a specific ssDNA oligomer, were flowed through different channels, and evaporated through the gas-permeable PDMS stamp, resulting in individual stripes of DNA molecules. One complete set of stripes represents one barcode. All measurements utilized 20  $\mu\text{m}$  wide bars spaced at 40  $\mu\text{m}$  pitch. This array density represents a  $\sim 10$ -fold increase over a typical spotted array (150  $\mu\text{m}$  spot diameters at 400  $\mu\text{m}$  pitch), thus expanding the numbers of proteins that can be measured within a small volume. No alignment between the barcode array and the plasma channels was required. All protein assays utilized one color fluorophore, and were spatially identified using a reference marker that fluoresced at a different color.

We first illustrate aspects of the barcode assays via the measurement of a single biomarker, human chorionic gonadotropin (hCG), in un-diluted human serum over a broad concentration range. hCG is widely used for pregnancy testing, and is a biomarker for gestational trophoblastic tumors and germ cell cancers of the ovaries and testes. For this assay, the barcode was customized by varying the DNA loading during the flow patterning step. The DNA barcode contained 13 regions (Fig. 2a). There were two bars of oligomer **B**, designed to detect the protein TNF $\alpha$  as a negative control. There was also one reference bar (oligomer **M**), one blank, and nine bars of oligomer **A** designed for hCG detection, flow patterned at ssDNA concentrations from 200 $\mu\text{M}$  to 2 $\mu\text{M}$ . To perform the assay, a mixture of **A**'-anti-hCG and **B**'-TNF- $\alpha$  was flowed through assay channels. Next, a series of standard hCG serum samples and two hCG samples of unknown concentration (provided by the National Cancer Institute) were flowed through separate assay channels. Biotinylated detection antibodies for hCG and TNF $\alpha$  were then applied, followed by a final developing step using fluorescent Cy5-labeled streptavidin (red) for all protein channels, and Cy3-labelled **M**' oligomers (green) for the reference channel (Fig. 2a). By quantitating the fluorescence intensity (Fig. 2b and c), a sensitivity ( $\sim 1\text{mIU/mL}$ ) comparable to the Enzyme-Linked Immunosorbent Assays (ELISAs) over a broad detected concentration range ( $\sim 10^5$ ), was demonstrated. Using the DEAL barcode in a blind test, we measured the hCG levels in

the two unknown serum samples. Our measured levels, estimated at 6 and 400mIU/mL for unknowns 1 and 2, are in good agreement with the values of 12 and 357 mIU/mL, respectively, obtained from an independent lab test (Labcorp, see Supplementary Fig. S5 online). Even without quantitation, the analyte concentrations can be estimated by eye through pattern-recognition of the full barcode. The bar with the highest DNA-loading rendered the highest sensitivity, whereas the bar with lowest DNA-loading was used to discriminate samples with high analyte concentrations. For example, the 25000mIU/mL and 250mIU/mL hCG samples can be visually distinguished using stripes patterned with lower DNA concentrations, whereas the stripes loaded with 200 $\mu$ M DNA look quite similar. For circumstances in which accurate photon counting is not available, visual barcode inspection permits a rough estimation of the target quantity — a potential point-of-care application. The level of hCG is tracked during pregnancy, with concentrations in the blood increasing from  $\sim$ 5mIU/mL in the first week of pregnancy to  $\sim$ 2 $\times$ 10<sup>5</sup> mIU/mL in ten weeks. The IBBC can cover such a broad physiological hCG range with reasonable accuracy.

We now describe multiplexed measurements of a panel of 12 protein markers using the DEAL barcode microfluidic chips. To evaluate the multiplexed assay, the cross-reactivity between the stripes within the DNA encoded immunoassays was quantitated. This test involved twelve human serum proteins, including ten cytokines (IFN- $\gamma$ , TNF- $\alpha$ , IL2, IL1 $\alpha$ , IL1 $\beta$ , TGF- $\beta$ 1, IL6, IL10, IL12, GMCSF), a chemokine (MCP-1) and a cancer biomarker (prostate specific antigen, PSA). The results showed a negligible cross-talk, with typical photon counts under 2% compared to the correctly paired antigen-antibody complexes (see Supplementary Fig. S8 on line). We also carried out assays on serial dilutions (from 5nM to 1pM) for these proteins on the DEAL barcode chip to establish a set of calibration curves for future estimates of protein concentration in sera. We fixed all the parameters associated with laser scanning and fluorescence quantification, i.e. power, gain, brightness, contrast, etc., and performed quantitative analysis as shown in Supplementary Fig. 9b online. The estimated sensitivity varies substantially depending upon the antibodies used, from <1pM for IL-1 $\beta$  and IL-12, to  $\sim$ 30pM for TGF- $\beta$ , and are comparable to the detection limits of ELISAs based on the same antibody pairs. For example, according to the specifications (eBioscience), the detection limit is  $\sim$ 8pg/mL, or 0.5pM for cytokines like TNF- $\alpha$  and IL1 $\beta$ , which is comparable to our observations. The statistical variation of the measured signals, however, is relatively large compared to a commercial ELISA assay — a variation that likely arises from our manual chip manufacturing processes.

We assessed the utility of the DEAL barcodes for clinical blood samples by measuring the panel of 12 proteins from small amounts of stored serum from 22 cancer patients. These serum samples were thawed, and then assayed using two chips, each containing 12 separate assay units operated in parallel. In every unit, 20 full DEAL barcodes in each assay channel were employed for statistical sampling. The proteins in this panel, the prostate cancer marker PSA, plus eleven proteins secreted by various white blood cells, have been found to have significant implications in tumor microenvironment formation, and in tumor progression and metastasis<sup>21-23</sup>. Thus, this panel provides information on both cancer and the immune system.

Fluorescence images, each showing four sets of (randomly picked) barcodes obtained from the 22 patient samples, are shown in Fig. 3b. The medical records for all patients are summarized (see Supplementary Table S3). B01-B11 denote 11 samples from breast cancer patients, P01-P11 are from prostate cancer patients. Many proteins were successfully detected with high signal-to-noise, and the barcode signatures are distinctive among patients. Assays show a high signal-to-background ratio, excepting the assays on P05, P04, P10 and B10, which were found from patients that were heavy smokers (~11-20cigs/day); only one serum sample from a heavy smoker did not exhibit a high background (P06). A possible cause of this high background is the elevated blood content of the fluorescent carboxyhemoglobin formed in lung<sup>24</sup>. While we have also measured high background in a number of stored serum samples, we have never measured a high background in assays from very freshly collected blood, as described below. The results imply that, at least for stored samples, some pre-purification of the plasma or serum will be required in order to assay serum protein levels.

Quantitation of barcode intensities were then carried out and the statistic mean value for each protein was computed (see Supplementary Fig. S11,S12).

The cancer marker, PSA, clearly distinguishes between the breast cancer and prostate cancer patients. The only exception is a false positive result from B10 that has high non-specific background. We independently validated our PSA measurements using the standard ELISA for PSA in all patient sera. For 8 of the prostate cancer patients, we compared these results with clinical ELISA measurements provided by the serum supplier (Asterand). The results (Fig. 3c), validate the applicability the DEAL barcodes for assaying complex clinical samples. However, the statistical accuracy of the PSA barcode assay was not high; only a modest linear correlation between the ELISA and DEAL (see Supplementary Fig. S10 online) was recorded. Again, this is likely due to our manual chip manufacturing process. We are currently automating our barcode fabrication, assay execution, and image quantitation in an effort to bring our statistical uncertainties to within 10-20%, which would be close to the state-of-the-art.

The cancer patient barcode data could be analyzed for absolute protein levels by comparing that data against the barcode quantitation plots (Supplementary Fig. S9 on line). Results for three proteins, PSA, TNF- $\alpha$  and IL1- $\beta$  are shown in Fig. 3d. PSA concentrations range from 22pM to 1nM (or 0.7 to 33ng/mL) with a log-scale mean of 117pM (3.8ng/mL) for prostate cancer patients. The estimated PSA concentrations for breast cancer patient sera has a mean of 9.1pM. PSA readily differentiates between these two patient groups with good statistical accuracy ( $p=0.0007$ ). Nevertheless, the absolute PSA levels measured by either the standard ELISA or by the barcode assay are below the clinical ELISA, a likely result of sample degradation during storage (Fig. 3c). As would be expected, neither TNF- $\alpha$  or IL-1 $\beta$  allows the separation of prostate and breast cancer patients ( $p=0.4$  and  $0.5$ , respectively at significance level  $0.2$ ). Our estimates of absolute protein levels indicate that the protein concentration ranges the DEAL barcode assay assesses are clinically relevant for patient diagnostics. For example, the serum level of cytokines such as interleukins and tumor necrosis factors can reach ~10-100pg/mL in cancer patients<sup>25</sup>, ~500pg/mL in rheumatoid

arthritis patients and  $>1\text{ng/mL}$ <sup>26</sup> in septic shock<sup>27</sup>. These levels can all be captured using the barcode assay format.

We performed a complete non-supervised clustering of patients on the basis of protein signals and generated the heat map (Fig. 3e) to assess the potential of this technology for patient stratification. This analysis is only presented as a proof-of-principle. Nevertheless, the results are encouraging. For example, the measured profiles of breast cancer patients can be classified into three subsets — non-inflammatory, IL-1 $\beta$  positive, and TNF- $\alpha$ /GMCSF positive ( $p_{\text{TNF}\alpha}=0.005$ ,  $p_{\text{GMCSF}}=0.04$  for the latter two subsets). The prostate cancer patient data were classified into two major subsets based upon the inflammatory protein levels ( $p_{\text{TNF}\alpha}=0.016$ ,  $p_{\text{GMCSF}}=0.012$ ). The multiplexed measurement of cytokines<sup>28</sup> has shown relevance in cancer diagnostics and prognostics<sup>29, 30</sup>. The results described demonstrate that IBBCs can be applied to the multiparameter analysis of human health-relevant proteins in serum.

The ultimate goal behind developing the IBBC was to measure the levels of a large number of proteins in human blood within a few minutes of sampling that blood, so as to avoid protein degradation that can occur when plasma is stored. In a typical 96 well plate immunoassay, the biological sample of interest is added, and the protein diffuses to the surface-bound antibody. Under sufficient flow conditions, diffusion is no longer important, and the only parameter that limits the speed of the assay is the protein/antibody binding kinetics (the Langmuir isotherm)<sup>31</sup>, thus allowing the immunoassay to be completed in just a few minutes<sup>32</sup> (see Supplementary §S.6 online). Flow through our plasma-skimming channels proceeds at velocities greater than  $\sim 0.1$  millimeter $\cdot$ sec<sup>-1</sup>, and can operate continuously and with near 100% efficiency unless the blood flow is clogged.

For whole blood analysis, the microfluidic channels of IBBCs were pre-coated with bovine serum albumin blocking buffer. The DNA barcodes were transformed into antibody barcodes as described above, and blood samples were flowed into the device within 1 minute of finger-prick collection. The time from that finger prick to completion of blood flow through the device was about 9 minutes. We sampled both as-collected whole blood and protein-spiked blood from healthy volunteers. For the unspiked blood, the collection tubes were pre-filled with 80  $\mu\text{L}$  of 25 mM EDTA solution. For protein-spiked blood samples, the collection tubes were filled with 40  $\mu\text{L}$  of 25 mM EDTA solution, 40  $\mu\text{L}$  of standard protein solution, and 2  $\mu\text{L}$  of 0.5M EDTA was added to bring the total EDTA concentration up to 25mM. Finger pricks were sampled using a miniaturized blood sampling kit (BD Microtainer Contact-Activated Lancets for low volume single blood drop). 10  $\mu\text{L}$  of Blood was collected with SAFE-T-FILL, EDTA-coated capillaries (RAM Scientific) and added to the prepared collection tubes. The diluted blood sample was then introduced onto the chip, and the skimmed plasma was flowed over the DEAL barcode region for 8 minutes. Fig. 4a shows the effective separation of plasma in an IBBC. The few red blood cells that did enter the plasma channels (Fig 4a, right panel) did not affect the subsequent protein assay

The plasma proteins that were detected in this experiment included a cancer marker — prostate specific antigen (PSA), four cytokines, and three other functional proteins (C3, CRP

and plasminogen) involved in the complement system, inflammatory response and fibrin degradation, as well as in liver toxicity (see Supplementary Tables S1,S2 online). After the whole blood was introduced into an IBBC, and plasma was flowed over the barcode zone for 8 minutes, the plasma proteins of interest were successfully captured. Then, the detection antibody solution and the fluorescence probes were added to complete the assay. As shown in Fig. 4b and 4c, all proteins in the spiked blood were detected (cytokines gave rise to the strongest fluorescence signals because of high antibody affinities). The measurement of the unspiked fresh blood established a baseline for a healthy volunteer, in which IL-6, IL-10, C3 and plasminogen were detected. Utilizing IBBCs for the separation and analysis of very freshly collected blood consistently resulted in very clean DEAL barcodes, with little or no evidence of biofouling. We are planning a study to assess the importance of rapid measurements for obtaining accurate protein levels.

The IBBC enables the rapid measurement of a panel of plasma proteins from a finger prick of whole blood. Integration of microfluidics and DNA-encoded antibody arrays enables reliable processing of blood and *in situ* measurement of plasma proteins within a time scale that is shorter than most blood chemistry that can degrade protein levels. Use of the IBBC represents a minimally invasive, low-cost, and robust procedure, and potentially represents a realistic clinical diagnostic platform.

## METHODS

### Micropatterning of barcode array

A polydimethylsiloxane (PDMS) mold containing 13-20 parallel microfluidic channels, with each channel conveying a different DNA oligomer as DEAL code, was fabricated by soft lithography. The PDMS mold was bonded to a polylysine-coated glass slide via thermal treatment at 80°C for 2 hours. The polyamine surfaces permit significantly higher DNA loading than do more traditional aminated surfaces. DNA “bars” of 2 micrometers in width have been successfully patterned using this technique. In the present study, a 20-micrometer ( $\mu\text{m}$ ) channel width was chosen because the fluorescence microarray scanner we used has a resolution of 5 $\mu\text{m}$ . Nevertheless, the current design already resulted in a DNA barcode array an order of magnitude denser than conventional microarrays fabricated by pin-spotting. The coding DNA solutions (A-M for the cancer serum test and AA-HH for the finger-prick blood test) prepared in 1xPBS were flowed into individual channels, and then allowed to evaporate completely. Finally, the PDMS was peeled off and the substrate with DNA barcode arrays was baked at 80°C for 2-4 hours. The DNA solution concentration was  $\sim 100\mu\text{M}$  in all experiments except in the hCG test, leading to a high loading of  $\sim 6 \times 10^{13}$  molecules/cm<sup>2</sup> (assuming 50% was collected onto substrate).

### Fabrication of IBBCs

The fabrication of PDMS devices for the IBBCs was accomplished through a two-layer soft lithography approach. The control layer was molded from a SU8 2010 negative photoresist ( $\sim 20\mu\text{m}$  in thickness) silicon master using a mixture of GE RTV 615 PDMS prepolymer part A and part B (5:1). The flow layer was fabricated by spin-casting the pre-polymer of GE RTV 615 PDMS part A and part B (20:1) onto a SPR 220 positive photoresist master at

~2000rpm for 1minute. The SPR 220 mold was ~17  $\mu\text{m}$  in height after rounding via thermal treatment. The control layer PDMS chip was then carefully aligned and placed onto the flow layer, which was still situated on its silicon master, and an additional 60min thermal treatment at 80°C was performed to enable bonding. Afterward, this two-layer PDMS chip was cut off the flow layer master and access holes were drilled. Finally, the tow-layer PDMS chip was thermally bonded onto the barcode-patterned glass slide (described above), yielding a completed integrated blood barcode chip (IBBC). In this chip, the DEAL barcode stripes are orientated perpendicular to the microfluidic assay channels. Typically, 8-12 identical units were integrated in a single chip with the dimensions of 2.5cm $\times$ 7cm.

### **Clinical specimens of cancer patient sera**

The stored serum samples from 11 breast cancer patients(all female) and 11 prostate cancer patients(all male) were acquired from Asterand. Nineteen out of 22 patients were Caucasian and the remaining three were Asian, Hispanic and African-American. The medical history is summarized in the supplementary materials.

### **Collecting a finger-prick of blood**

The human whole blood was collected according to the protocol approved by the Institutional Review Board of California Institute of Technology. Finger pricks were performed using BD Microtainer Contact-Activated Lancets. Blood was collected with SAFE-T-FILL capillary blood collection tubes (RAM Scientific), which we pre-filled with 80  $\mu\text{L}$  of 25 mM EDTA solution. A 10  $\mu\text{L}$  volume of fresh human blood from a healthy volunteer was collected in this EDTA-coated capillary, dispensed into the tube, and rapidly mixed by inverting a few times. The spiked blood sample was prepared in a similar means except that 40  $\mu\text{L}$  of 25 mM EDTA solution and 40  $\mu\text{L}$  of recombinant solution were mixed and pre-added in the collection tube. Then 2  $\mu\text{L}$  of 0.5 M EDTA was added to bring the total EDTA concentration up to 25mM.

### **Execution of blood separation and plasma protein measurement using IBBCs**

—The IBBCs were first blocked with the buffer solution for 30-60 minutes. The buffer solution prepared was 1% w/v Bovine Serum Albumin Fraction V (Sigma) in 150 mM 1x PBS without calcium/magnesium salts (Irvine Scientific). The fluid loading was conducted using a Tygon® plastic tubing that is interfaced to the IBBC inlet with a 23 gauge metal pin. The Fluidigm® solenoid unit was exploited to control the pressure on/off for both control valves and flow channels. A pressure of 8-10 psi was applied to actuate the valves, whereas the loading of fluid into assay channels was carried out with a lower pressure (0.5-3psi) depending on the channel flow resistance and the desired flow rate. Then DNA-antibody conjugates (~50-100nM) were flowed through the plasma assay channels for ~30-45min. This step transformed the DNA arrays into capture-antibody arrays. Unbound conjugates were washed off by flowing buffer solution through the channels. At this step, the IBBC was ready for the blood test. Two blood samples prepared as mentioned above were flowed into the IBBCs within 1 minute of collection. The IBBC quickly separated plasma from whole blood, and the plasma proteins of interest were captured in the assay zone where DEAL barcode arrays were placed. This whole process from finger-prick to plasma protein capture took <10 minutes. In the cancer-patient serum experiment, the as-received serum samples



were flowed into IBBCs without any pre-treatment (i.e. no purification or dilution). Afterwards, a mixture of biotin-labeled detection antibodies (~50-100nM) for the entire protein panel and the fluorescence Cy5-straptavidin conjugates (~100nM) were flowed sequentially into IBBCs to complete the DEAL immunoassay. The unbound fluorescence probes were rinsed off by flowing the buffer solution for 10 minutes. At last, the PDMS chip was removed from the glass slide. The slide was immediately rinsed in 1/2 x PBS solution and deionized water, and then dried with a nitrogen gun. Finally, the DEAL barcode slide was scanned by a microarray scanner.

### Quantitation and statistics

All the barcode array slides used in quantation were scanned using an Axon Genepix 4000B two-color laser microarray scanner at the same instrumental settings —100% and 33% for the laser power of 635nm and 532nm, respectively. Optical gains are 800 and 700 for 635nm and 532nm, respectively. The brightness and contrast were set at 87 and 88. The output JPEG images were carefully skewed and resized to fit the standard mask design of barcode array. Then, an image processing software, NIH imageJ, was employed to produce intensity line profiles of barcodes in all assay channels. Finally, all the line profile data files were loaded into home-developed program embedded as an excel macro to generate a spread sheet that lists the average intensities of all 13 bars in each of 20 barcodes. The means and standard divisions were computed using the Microcal origin. Non-supervised clustering of patients was performed using the software *Cluster* and the heat map was generated from the software *Treeview*, both developed by the M. Eisen's group. To assess the significance of two patient (sub)groups, student t analysis was performed on selected proteins and all p-values were calculated at significance level of 0.05 if not specified.

### Supplementary Material

Refer to Web version on PubMed Central for supplementary material.

### ACKNOWLEDGEMENTS

The authors thank Larry Nagahara and Chris Mcleland at the National Cancer Institute (NCI) for providing standard hCG serum samples and requesting the independent hCG measurement. We also thank Bruz Marzolf at the Institute for Systems Biology (Seattle, WA) for printing DNA microarrays, and the UCLA nanolab for photomask fabrication. This work was funded by the National Cancer Institute Grant No. 5U54 CA119347 (J.R.H., P.I.) and by the Institute for Collaborative Biotechnologies through grant DAAD19-03-D-0004 from the U.S. Army Research Office.

### REFERENCES

1. Anderson NL, Anderson NG. The human plasma proteome - History, character, and diagnostic prospects. *Molecular & Cellular Proteomics*. 2002; 1:845–867. [PubMed: 12488461]
2. Fujii K, et al. Clinical-scale high-throughput human plasma proteome clinical analysis: Lung adenocarcinoma. *Proteomics*. 2005; 5:1150–1159. [PubMed: 15712241]
3. Lathrop JT, Anderson NL, Anderson NG, Hammond DJ. Therapeutic potential of the plasma proteome. *Current Opinion in Molecular Therapeutics*. 2003; 5:250–257. [PubMed: 12870434]
4. Chen JH, et al. Plasma proteome of severe acute respiratory syndrome analyzed by two-dimensional gel electrophoresis and mass spectrometry. *Proceedings of the National Academy of Sciences of the United States of America*. 2004; 101:17039–17044. [PubMed: 15572443]

5. Hsieh SY, Chen RK, Pan YH, Lee HL. Systematical evaluation of the effects of sample collection procedures on low-molecular-weight serum/plasma proteome profiling. *Proteomics*. 2006; 6:3189–3198. [PubMed: 16586434]
6. Sia SK, Whitesides GM. Microfluidic devices fabricated in poly(dimethylsiloxane) for biological studies. *Electrophoresis*. 2003; 24:3563–3576. [PubMed: 14613181]
7. Quake SR, Scherer A. From micro- to nanofabrication with soft materials. *Science*. 2007; 315:81–84. [PubMed: 17204646]
9. Ottesen EA, Hong JW, Quake SR, Leadbetter JR. Microfluidic digital PCR enables multigene analysis of individual environmental bacteria. *Science*. 2006; 314:1464–1467. [PubMed: 17138901]
10. Huang LR, Cox EC, Austin RH, Sturm JC. Continuous particle separation through deterministic lateral displacement. *Science*. 2004; 304:987–990. [PubMed: 15143275]
11. Chou CF, et al. Sorting biomolecules with microdevices. *Electrophoresis*. 2000; 21:81–90. [PubMed: 10634473]
12. Toner M, Irimia D. Blood-on-a-chip. *Annual Review of Biomedical Engineering*. 2005; 7:77–103.
13. Nagrath S, et al. Isolation of rare circulating tumour cells in cancer patients by microchip technology. *Nature*. 2007; 450:1235–U1210. [PubMed: 18097410]
14. Yang S, Undar A, Zahn JD. A microfluidic device for continuous, real time blood plasma separation. *Lab on a Chip*. 2006; 6:871–880. [PubMed: 16804591]
15. Svanes K, Zweifach BW. Variations in small blood vessel hematocrits produced in hypothermic rates by micro-occlusion. *Microvascular Research*. 1968; 1:210–220.
16. Fung YC. Stochastic flow in capillary blood vessels. *Microvasc. Res*. 1973; 5:34–38. [PubMed: 4684755]
17. Bailey RC, Kwong GA, Radu CG, Witte ON, Heath JR. DNA-encoded antibody libraries: A unified platform for multiplexed cell sorting and detection of genes and proteins. *Journal of the American Chemical Society*. 2007; 129:1959–1967. [PubMed: 17260987]
18. Boozer C, Ladd J, Chen SF, Jiang ST. DNA-directed protein immobilization for simultaneous detection of multiple analytes by surface plasmon resonance biosensor. *Analytical Chemistry*. 2006; 78:1515–1519. [PubMed: 16503602]
19. Niemeyer CM. Functional devices from DNA and proteins. *Nano Today*. 2007; 2:42–52.
20. Pirrung MC. How to make a DNA chip. *Angewandte Chemie-International Edition*. 2002; 41:1277–+.
21. Coussens LM, Werb Z. Inflammation and cancer. *Nature*. 2002; 420:860–867. [PubMed: 12490959]
22. Lin WW, Karin M. A cytokine-mediated link between innate immunity, inflammation, and cancer. *Journal of Clinical Investigation*. 2007; 117:1175–1183. [PubMed: 17476347]
23. De Marzo AM, et al. Inflammation in prostate carcinogenesis. *Nature Reviews Cancer*. 2007; 7:256–269. [PubMed: 17384581]
24. Ashton H, Telford R. Smoking and carboxhemoglobin. *Lancet*. 1973; 2:857–858. [PubMed: 4126663]
25. Chopra V, Dinh TV, Hannigan EV. Serum levels of interleukins, growth factors and angiogenin in patients with endometrial cancer. *Journal of Cancer Research and Clinical Oncology*. 1997; 123:167–172. [PubMed: 9119882]
26. Oncul O, Top C, Cavuplu P. Correlation of serum leptin levels with insulin sensitivity in patients with chronic hepatitis-C infection. *Diabetes Care*. 2002; 25:937–937. [PubMed: 11978698]
27. Pinsky MR, et al. SERUM CYTOKINE LEVELS IN HUMAN SEPTIC SHOCK - RELATION TO MULTIPLE-SYSTEM ORGAN FAILURE AND MORTALITY. *Chest*. 1993; 103:565–575. [PubMed: 8432155]
28. Schweitzer B, et al. Multiplexed protein profiling on microarrays by rolling-circle amplification. *Nature Biotechnology*. 2002; 20:359–365.
29. Lambeck AJA, et al. Serum cytokine profiling as a diagnostic and prognostic tool in ovarian cancer: A potential role for interleukin 7. *Clinical Cancer Research*. 2007; 13:2385–2391. [PubMed: 17438097]

30. Gorelik E, et al. Multiplexed immunobead-based cytokine profiling for early detection of ovarian cancer. *Cancer Epidemiology Biomarkers & Prevention*. 2005; 14:981–987.
31. Heath JR, Davis ME. Nanotechnology and cancer. *Annual Review of Medicine*. 2007; 59:405.
32. Zimmermann M, Delamarche E, Wolf M, Hunziker P. Modeling and optimization of high-sensitivity, low-volume microfluidic-based surface immunoassays. *Biomedical Microdevices*. 2005; 7:99–110. [PubMed: 15940422]

Author Manuscript

Author Manuscript

Author Manuscript

Author Manuscript

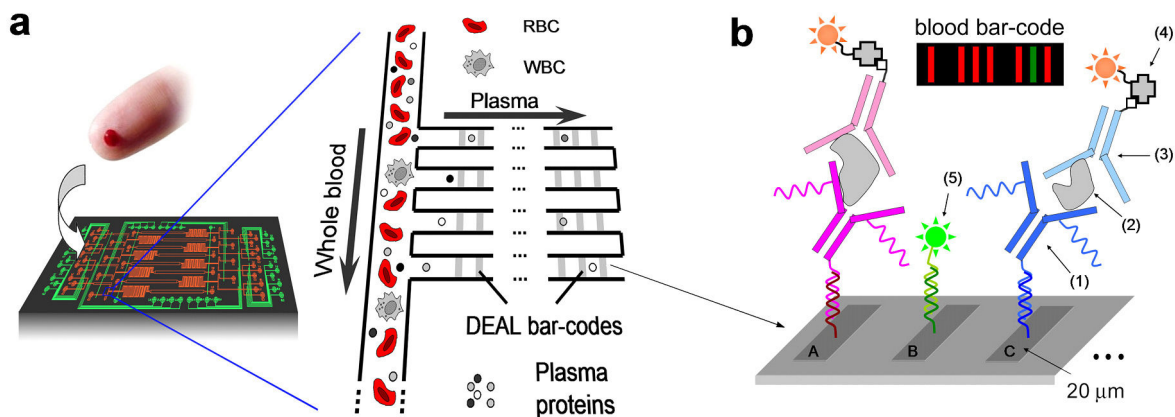


**Figure 1.** Design of an integrated blood barcode chip (IBBC). **(a)** Scheme depicting plasma separation from a fingerprick of blood by harnessing the Zweifach-Fung effect. Multiple DNA-encoded antibody barcode arrays are patterned within the plasma skimming channels for *in situ* protein measurements. **(b)** Illustration of DEAL barcode arrays patterned in plasma channels for *in situ* protein measurement. A, B, C indicate different DNA codes. (1)-(5) denote DNA-antibody conjugate, plasma protein, biotin-labeled detection antibody, streptavidin-Cy5 fluorescence probe, and complementary DNA-Cy3 reference probe, respectively. The inset represents a barcode of protein biomarkers, which is read out using fluorescence detection. The green bar represents an alignment marker.

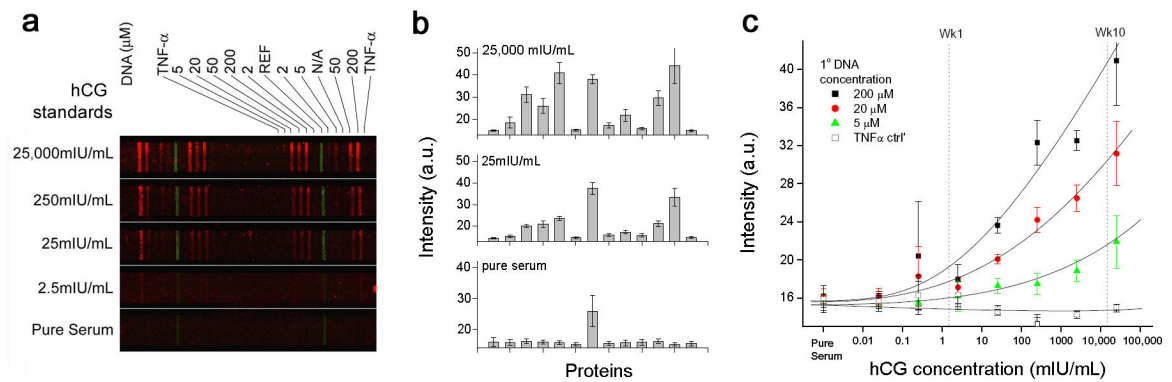


**Figure 2.**

Measurement of human chorionic gonadotropin (hCG) in sera. **(a)** Fluorescence images of DEAL barcodes showing the measurement of a series of standard serum samples spiked with hCG. The bars used to measure hCG were patterned with DNA strand **A** at different concentrations. TNF- $\alpha$  encoded by strand **B** was employed as a negative control. The green bars (strand **M**) serve as references. **(b)** Quantification of the full barcodes for three selective samples. **(c)** Mean values of fluorescence signals corresponding to three sets of bars with different DNA loadings. The dash lines indicate the typical physiological levels of hCG in sera after one or ten weeks of pregnancy. The length of error bars represents 1SD.

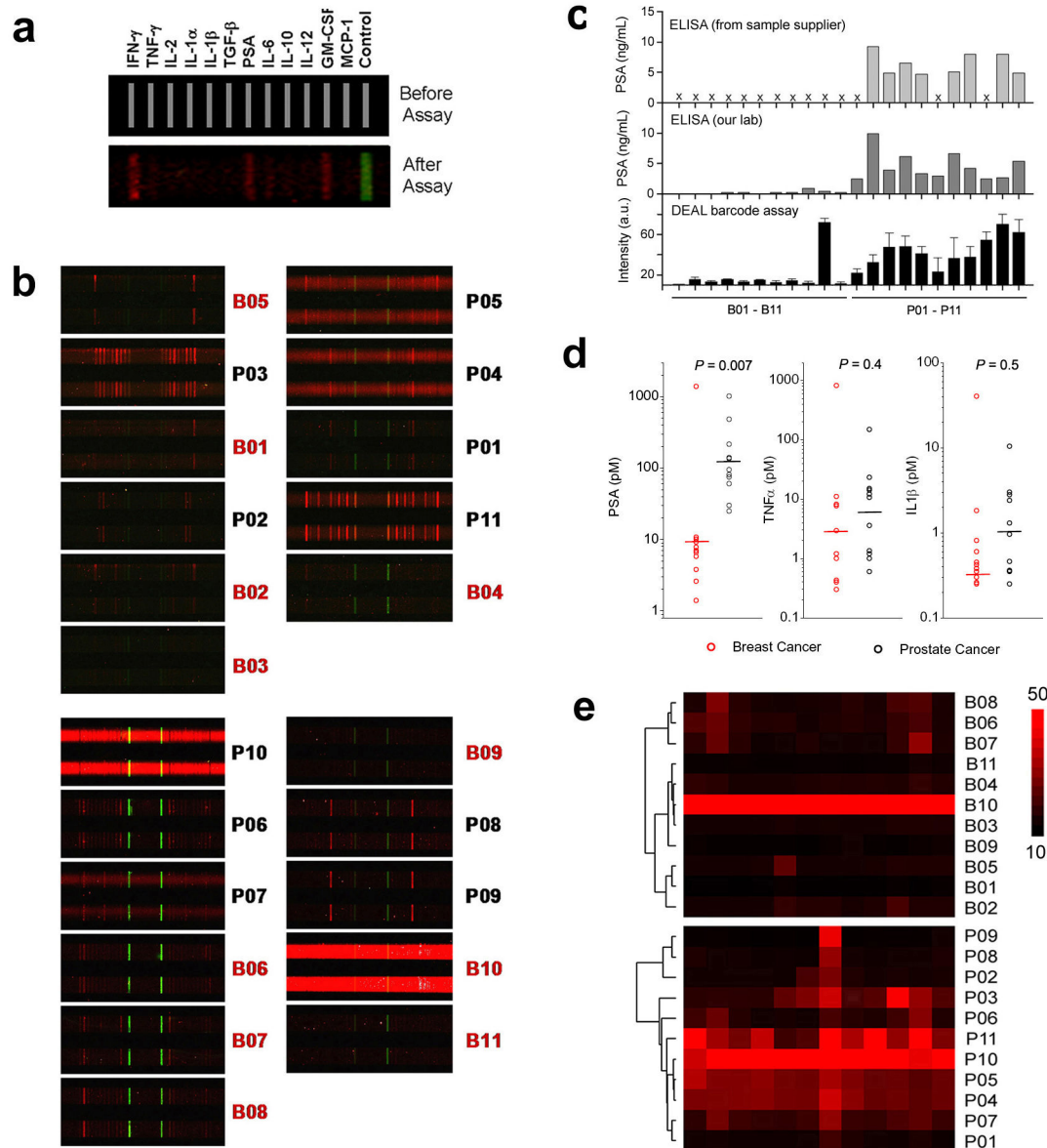


**Figure 3.** Multiplexed protein measurements of clinical patient sera. **(a)** Layout of the barcode array used in this study. Green denotes the reference (strand M). **(b)** Representative fluorescence images of barcodes used in measuring a dozen proteins (the cancer marker PSA and eleven cytokines) from 22 cancer patient serum samples. B01-B11 denote breast cancer patients, P01-P11 denote prostate cancer patients. The left and right columns represent measurements on different chips. **(c)** Validation of PSA DEAL barcode measurement using ELISA (x denotes PSA measurements were not provided by the serum supplier) (Error bar: 1 standard deviation). **(d)** Distribution of estimated concentrations of PSA, TNF $\alpha$  and IL1 $\beta$  in all serum samples. The horizontal bars mark the mean values. **(e)** Complete non-supervised clustering of breast and prostate cancer patients on the basis of protein patterns.

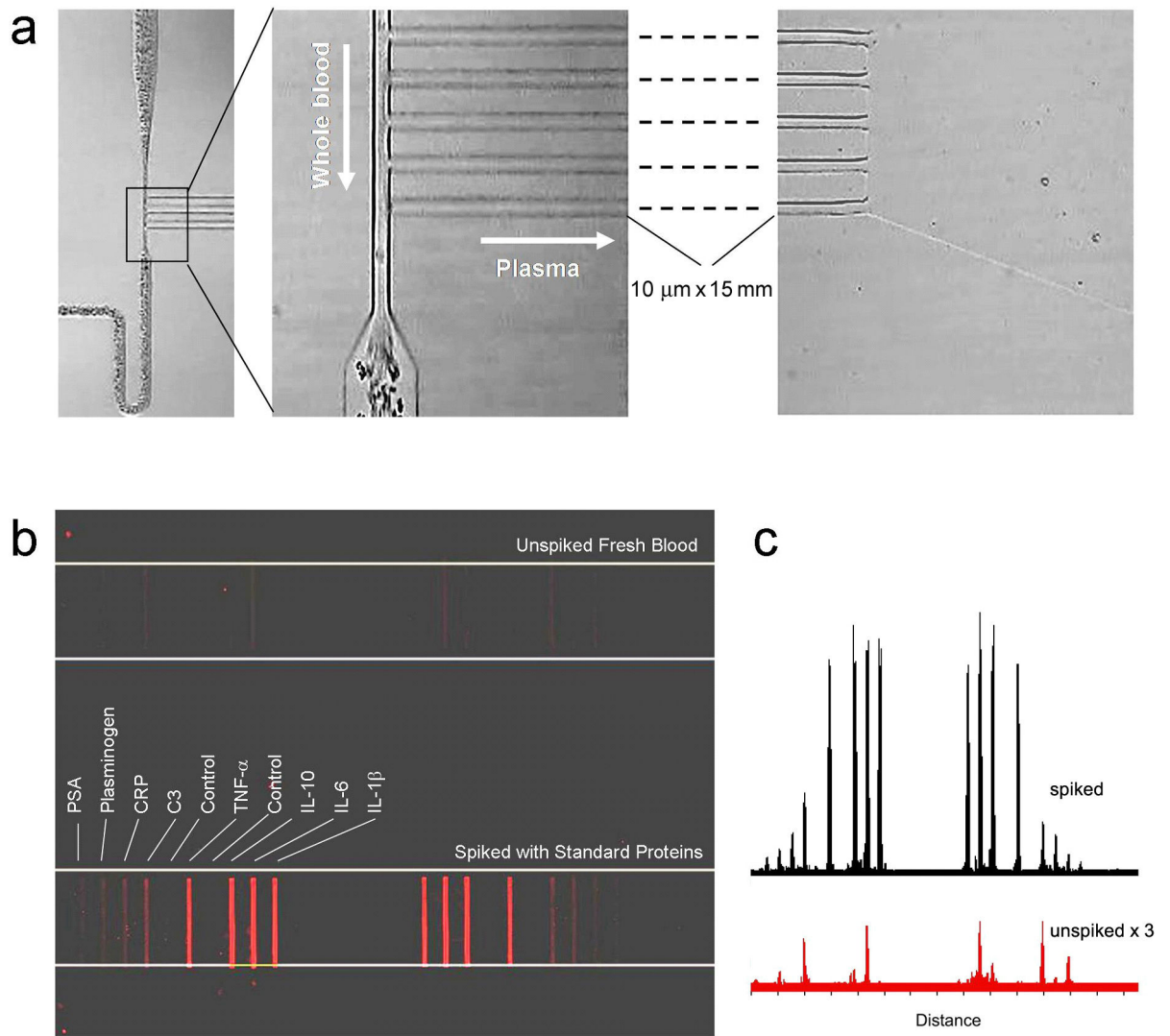


**Figure 4.**

IBBC for the rapid measurement of a panel of serum biomarkers from a finger-prick of whole blood. (a) Optical micrographs showing the effective separation of plasma from fresh whole blood. A few red blood cells were occasionally seen downstream of the plasma channels, but this did not